Compressed Sensing Based Spherical Mode Filtering Reflection Suppression for Far-Field Testing in Complex Electromagnetic Environments

S.F. Gregson[1, 2], R. F. Dubrovka[1], C.G. Parini[1]
[1] School of Electronic Engineering and Computer Science, Queen Mary University of London, London, UK, r.dubrovka@qmul.ac.uk
[2] Next Phase Measurements Ltd., Garden Grove, CA, USA, stuart.gregson@npmeas.com

***Abstract*—This paper presents the first investigation of a two-dimensional, compressed sensing based spherical mode filtering reflection suppression technique for far-field antenna measurements when applied in a complex electromagnetic environment, *e.g.* when the test antenna is in the presence of a an electrically large parasitically coupled scatterer. Such scatterers inevitably influence measurement results including radiation pattern, cross-polarisation level, gain, directivity, *etc.*, and are of particular concern when testing in a far-field mode; and especially so when testing outside. Through a massive numerical simulation which utilised a proprietary full-wave, three-dimensional, computational electromagnetic solver, the viability of this new processing technique has been verified, with preliminary results showing that the technique is valid even under such complex scattering conditions.**

***Index Terms*—Model based systems engineering, compressed sensing, sparse sampling, reflection suppression, mode filtering, full-wave computational electromagnetic simulation.**

I. Introduction

In many applications, we are required to acquire the full two-dimensional far-field pattern of an antenna under test (AUT) while adhering to the standard spherical sampling theorem [1]. Often, these measurements are undertaken in an indoor, screened, anechoic chambers at a far-field distance, or within a Compact Antenna Test Range (CATR). So as to be able to reduce the inevitable effects of range multipath reflections, *i.e.,* the presence of deleterious parasitically coupled scatterers, it is well known that that by rotating the antenna under test with an intentional positional offset, and subsequently applying a mathematical translation on the measured pattern data to translate the antenna back to the rotation centre, it is possible to filter out the higher order modes that are associated with the parasitically coupled multipath [1]. When the measurement is performed on an equally spaced abscissa, the conversion from the two-dimensional angular domain to the equivalent spherical mode domain can be efficiently computed by first decomposing the tangential orthogonal electric field components onto a set of Fourier coefficients which can be accomplished efficiently by means of the mixed-radix Fast Fourier Transform (FFT) [2]. These Fourier coefficients can then be mapped onto a set of spherical mode coefficients (SMC) whereupon the mode filtering, *etc.* can be applied [1].

It is, however, not always convenient or perhaps possible to acquire the data precisely on a plaid, monotonic, and equally-spaced, periodic, angular grid. This may be because of equipment accuracy limitations, or as a result of time constraints. This becomes all the more crucial when these measurements are taken using out-door facilities, which is often the case when testing electrically large antennas where the far-field distance is sufficiently great to make indoor testing uneconomical [1]. Additionally, such outdoor tests are also prone to limited stability making rapid acquisitions even more important. Furthermore, after stability, range reflections and multipath are perhaps the next most significant terms within the facility level uncertainty budget making the application of effective reflection suppression to sparsely sampled, irregularly sampled data particularly desirable [1]. In reference [3], one of the authors of this present paper demonstrated that for the case of scattering contaminated far-field one-dimensional data, it was possible to obtain the requisite cylindrical mode coefficients (CMC) by solving a system of simultaneous equations using a compressive sensing (CS) based sparse sampling (SS) technique. This suggested that a similar approach may perhaps be harnessed for the two-dimensional analogue which is the focus of this paper.

To verify the viability of this new approach, a large, computationally intensive, simulation campaign has been employed. The first results of which are presented in this paper. The layout of this paper is as follows; Section II presents an overview of the novel spherical mode CS based reflection suppression technique. This is followed by Section III which is mainly devoted to describing the simulated "measurement" setup, which was used for the numerical experiment simulations. Also, in this Section, the obtained results are explained in detail, whilst Section IV demonstrates the validity of the new sparse sampling, spherical mode filtering, based scattering suppression technique which was utilized to predict characteristics of the AUT in the complex electromagnetic environment. The paper is finalised by Conclusions, Acknowledgements and References.

978-88-31299-10-7/25/$31.00 ©2025 IEEE

II. Overview of CS Based Spherical Mode Filtering Algorithm

To accurately recover the modes associated with the antenna, the Nyquist sampling requirement states that the data density should, on average, be sufficiently great to accommodate any significant higher order modes, including those arising from the parasitically coupled scatterers [1]. This prevents aliases from contaminating the computed antenna modes. Furthermore, unevenly sampled data can usually result in spectrum leakage [3]. This occurs as a result of the Fourier basis losing its orthogonality when the sampling grid becomes irregular. This is one of the principal advantages of the CS approach in this area of application, since at its very heart, it inherently *requires* the samples to be taken on an irregular grid. In those earlier works [1, 3] it was also shown that when utilising the mode filtering scheme described above, the antenna modes occupy only the lowest order modes since the coordinate translation to relocate the AUT to the origin of the measurement coordinate system effectively reduces the Maximum Radial Extent (MRE). This is a conceptual sphere that circumscribes the majority of the current sources, and which is originated at the rotation centre. As a result, the number of modes containing a significant amount of power is greatly reduced since, according to theory, the mode cut-off is determined by the electrical size of the MRE. In other words, the relevant modes are sparsely distributed which enables the problem to be treated as a Compressed Sensing (CS) recovery problem [3]. With the SMCs recovered, a filtering function can be applied to preserve those modes that are associated with the physical dimension of the antenna [1, 3], whilst attenuating the effects of spurious reflections in the environment which appear as additional parasitic sources [1, 3].

Recent advancements in CS algorithms [4, 5] have made it possible to effectively solve such problems which classically have been considered to be underdetermined. Compressed Sensing can leverage the sparsity of data in the Fourier basis by aiming for a parsimonious solution that contains the smallest number of non-zero coefficients. By formulating the problem in terms of CS, we not only reduce the number of required sampling points (which can be far fewer than what is prescribed by the classical Nyquist criterion), but crucially, we eliminate the need for data to be collected regularly on the equispaced, two-dimensional spherical sampling grid. In fact, as noted above, random or pseudo-random sampling becomes essential. Our purpose here is to demonstrate that the CS algorithm can effectively reconstruct the antenna patterns, even with significantly relaxed sampling requirements and in the presence of a large parasitically coupled scatterer. The utilization of the CS approach in mode-filtering based reflection suppression applications as is employed here significantly broadens its applicability, enabling sub-Nyquist sampling and considerably reducing the requirements for positioning equipment accuracy, although requirements for precision still persist. The next section introduces the computational electromagnetic model that was constructed and used to verify the feasibility of this new technique.

III. The Numerical Experiment Setup

To create a numerical model of the requisite experiment, a proprietary, full-wave, three-dimensional computational electromagnetic solver Altair Feko [10] was utilised. To have a benchmark for obtained results, a model of 48-element finite antenna array has been used as an AUT [6] at 3.5 GHz. This radiator was perturbed with the inclusion of a perfect electric conducting (PEC) square plate and was used to create the complex environment. This can be seen presented below in Fig. 1 which replicated the positioning employed by a traditional "model tower" ϕ over θ spherical positioning system [1].

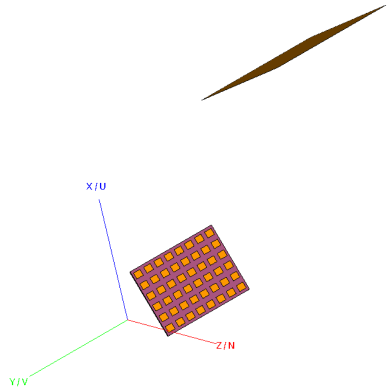

Fig. 1. The "measurement" setup, the AUT is on the left, and the scatterer is on the top of the figure.

Here we see on the left, the AUT is placed 360mm from the origin of the simulated spherical "measurement" setup. Also, in Fig. 1, the AUT can be seen positioned at $\theta = 30°$, *i.e.* offset from its nominally "normal" position. It is specially demonstrated here to illustrate the simulated measurement movement of the AUT in θ-direction during the parametric studies. On the right, a large PEC scatterer is placed. Its centre is positioned 1000mm up and right from the global coordinate system origin. This PEC plate has dimensions 400x400 mm which is larger than the array antenna. It is worth to mention that the scatterer is positioned orientated at approximately 25° to the *y-z* plane, to achieve a maximum effect in disturbing far-field pattern of the AUT. As in reference [6], the AUT was excited by an ideal network with equal amplitude and phase at all input ports. In the present case, the excitation is not a matter of the investigation, however, the complex nature of the field distribution makes it more attractive than a simple antenna even with a large aperture. Radiation characteristics of the AUT can be found in the same papers previously published by the authors [6].

The simulated experiment required that this model be solved multiple times to obtain the perturbed "measured" radiation pattern. Thus, the AUT was sequentially repositioned within the model to represent measurements taken at a range of (θ,ϕ) orientations where these angles are expressed in the range coordinate system. This simulated far-field measurement then required that the far-field pattern of the model be obtained in the "boresight" direction at θ = 0°, ϕ = 0° in the global coordinate system, shown in Fig. 1. for *every* position of the AUT in "measurement" spherical coordinate system. Thus, the AUT should sequentially move across all values of θ in *x-z* plane. For every such θ position the AUT is rotated around the normal to the AUT, changing value of ϕ from -180° to 177°. Using a step of 3° this yields 7320 points to be "measured", *i.e.*, 7320 individual method of moment (MoM) simulations. Although the CS technique does not need this much data, by simulating a classically sampled measurement it allow us the ability to process the data using classical, *i.e.*, standard, spherical mode filtering techniques [1] and provides a large ensemble of measurement from which we may select a smaller set of data to use with the CS processing. Furthermore, as CS is inherently a statistical process, we wish to run the processing many times with different sample sets to be able to determine meaningful metrics for its performance which this enables.

As was noted above, the simulation of a full measurement campaign requires extended simulation times and yields huge amounts of data. To check the configuration of the setup, and its connection to our physical understanding of the process, a simple case was first modelled for which the AUT was moved only along θ, keeping polarization of the AUT fixed, *i.e.*, not rotating along the AUT normal. The result of that simulation is shown in Fig. 2. Here, one can clearly see that the scatterer brings a very strong effect towards the boresight of the AUT when the AUT is rotated to approximately 45° from the original position and confirms that the scattering effects will be visible in the full measurement simulation.

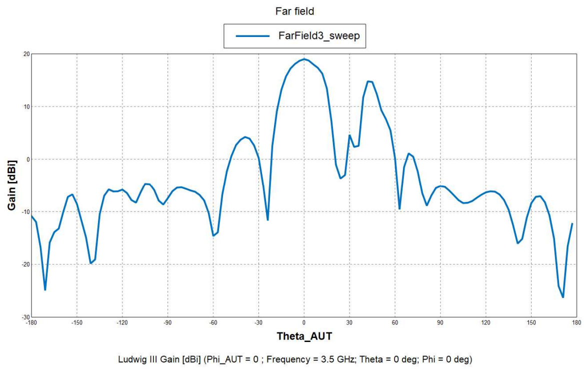

Fig. 2. Simulated far-field pattern cut for a single AUT θ-position showing the pattern is perturbed by the presence of the PEC scatterer.

Fig. 3 presents the aggregated results of these simulation for three ϕ-cuts at θ = 60°, 63°, and 66° which constitutes a total of 360 individual full-wave MoM simulations. These cuts will be further used within the sparse sampling simulations. These cuts present far-field, polar-spherical gain patterns of the AUT as a function of the rotation around the normal of the AUT for fixed θ-positions, *i.e.*, with ϕ = -180°, -177°, 174°…177°. Here, one can see how changing the orientation of AUT position affects radiation characteristic of antenna and simulates a classical, polar spherical, E_θ, E_ϕ measurement [1] where here the results are greatly impacted by the presence of the PEC scatterer.

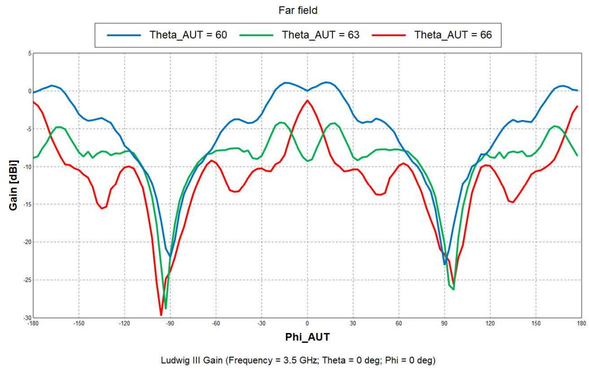

Fig. 3. Simulated far-field "measurement" results for three ϕ-cuts.

IV. Sparse Sampling Spherical Transform

Fig. 4 shows the sparsely sampled simulated measurement points that are used by the CS algorithm. Here, just 8% of the points what would be used by the full conventional equispaced spherical processing are required. These few samples are taken based on a cosine distribution of points in θ which varies from 0° to 90° where, for each θ point, we randomly select a ϕ point between -180° and +177°. This provides the necessary weighting with more samples placed in the region with greater field intensities around the spherical measurement pole, and which significantly improves the performance of the CS technique [7].

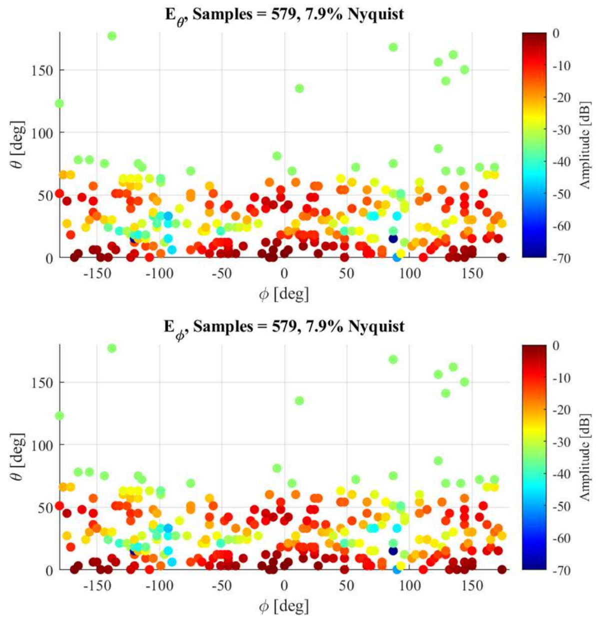

Fig. 4. Sparse spherical simulated "measured" data, top E_θ, bottom E_ϕ.

As noted above, the first step in the classical processing is to decompose the measured fields onto Fourier coefficients by means of a two-dimensional Fourier transform [2]. Fig. 5a and b shows the two sets of Fourier coefficients, one for each orthogonal polarisation, which have been computed conventionally using a mixed-radix two-dimensional FFT [2]. By contrast, Fig. 5c and d, presents equivalent results only here the Fourier coefficients have been computed using a CS based solver, *cf.* [8]. For the purposes of the CS recovery, it is the Fourier coefficients are the primary parameters of interest. The standard spherical near-field to far-field transform will take these recovered Fourier coefficients and map them onto spherical mode coefficients which are required to perform the spherical near-field to far-field transform and probe compensation [2].

To reduce the computational intensity and machine resources, a novel technique has been utilised that drastically reduces the size of the problem space. From inspection of Fig. 5a and b we see that very little power is contained within a cruciform region of the Fourier domain. In the linear-algebra statement, we may therefore exclude this region and instead limit our domain to the region in which Fourier coefficients that are associated with the AUT and the parasitically coupled scatterer are expected to reside. It is however crucial to the success of the technique to include the parasitically coupled coefficients as failure to do so means that their power will be aliased back into the AUT modes invalidating the technique.

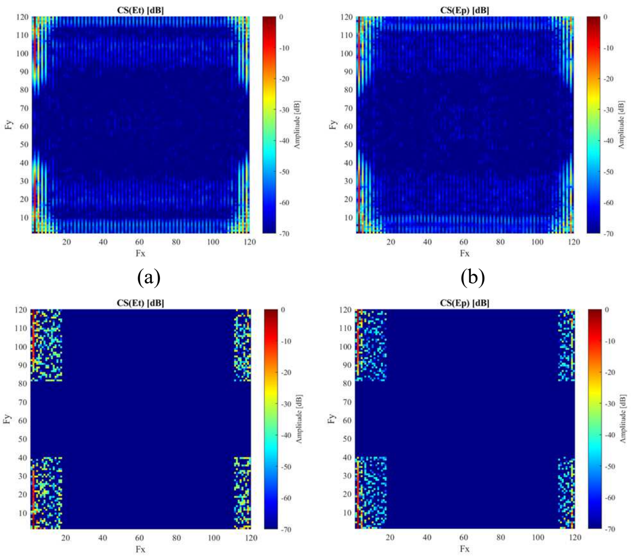

(a) (b) (c) (d)

Fig. 5. Fourier coefficients computed by conventional spherical processing (a) and (b), and equivalent results obtained by CS processing (c) and (d).

From inspection, we see that the agreement attained between those coefficients that were determined by employing a conventional Fourier transform, *i.e.* Fig. 5a and b are in very encouraging agreement with the equivalent results obtained by the CS solver, Fig. 5c and d. The next step in the standard spherical processing is to map these Fourier coefficients onto the spherical mode coefficients (SMC). Fig. 6a and b contain SMC plots for the TE and TM mode sets that were obtained using the standard processing. Conversely, Fig. 6c and d contain equivalent SMC plots that were obtained by mapping the CS derived Fourier coefficients onto SMCs. Here, the θ component Fourier coefficients are mapped onto the Q_2 SMCs and the ϕ component Fourier coefficients are mapped onto the Q_1 SMCs. Again, the agreement is very encouraging. In both cases the higher order modes that are associated with the parasitically coupled scatterer have been filtered out from these results leaving just those lower order AUT modes [1, 3].

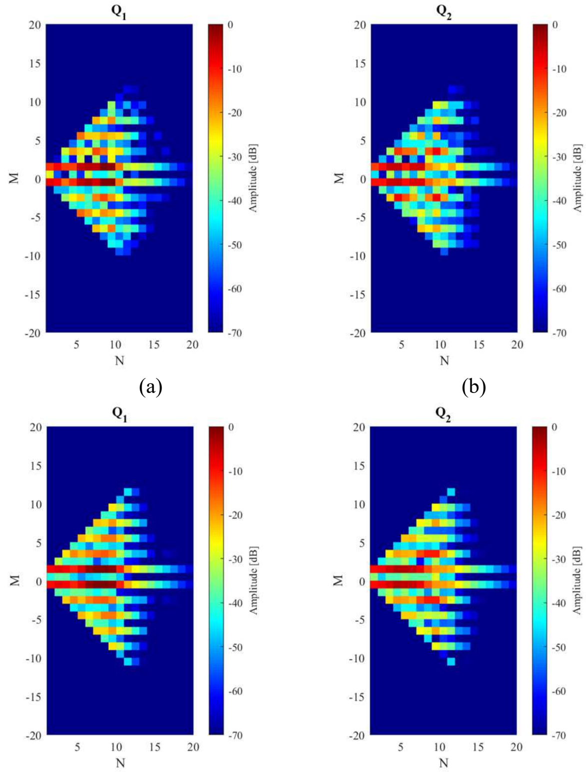

(a) (b) (c) (d)

Fig. 6. Spherical mode coefficients computed by mapping the Fourier coefficients onto the SMCs using standard spherical processing (a) and (b), and CS based processing (c) and (d).

The final step in the processing is to compute the equivalent, filtered, far-fields from the SMCs [2]. The far-field results can be seen presented below in Fig. 7. Fig. 7a and b contain the far-field co-polar and cross-polar Ludwig 3 [1] amplitude pattern of the unperturbed 3.5 GHz array antenna when tabulated on a regular azimuth over elevation coordinate system [1] and presented as a false colour checkerboard plot. Conversely, Fig. 7c and d contain equivalent plots for the case where the PEC reflecting plate has been introduced into the simulated "measurement" of the array antenna. Here we see the presence of very large spurious sidelobes, which are evident in both the co-polar and cross-polar patterns, which are a result of the very large specular reflection of the antenna in the PEC plate. Fig 7e and f contain the conventional reflection supressed, *i.e.*, mode filtered, far-field as obtained from using classical, that is to say non-CS, spherical processing [1]. Here, we see that the large amplitude spurious sidelobes have been greatly reduced, as is expected. Finally, Fig. 7g and h contain equivalent results for the novel CS based reflection suppression which are in close agreement with the results obtained from using classical spherical mode filtering. When interpreting these results, it is important to recognise that, as a consequence of limited processing time, "measured" spherical data was only available out to 60° in θ meaning that azimuth and elevation pattern angles larger than ±60° may be disregards as any fields outside of this range will differ from the true far-field antenna pattern by virtue of the first order truncation effect [1].

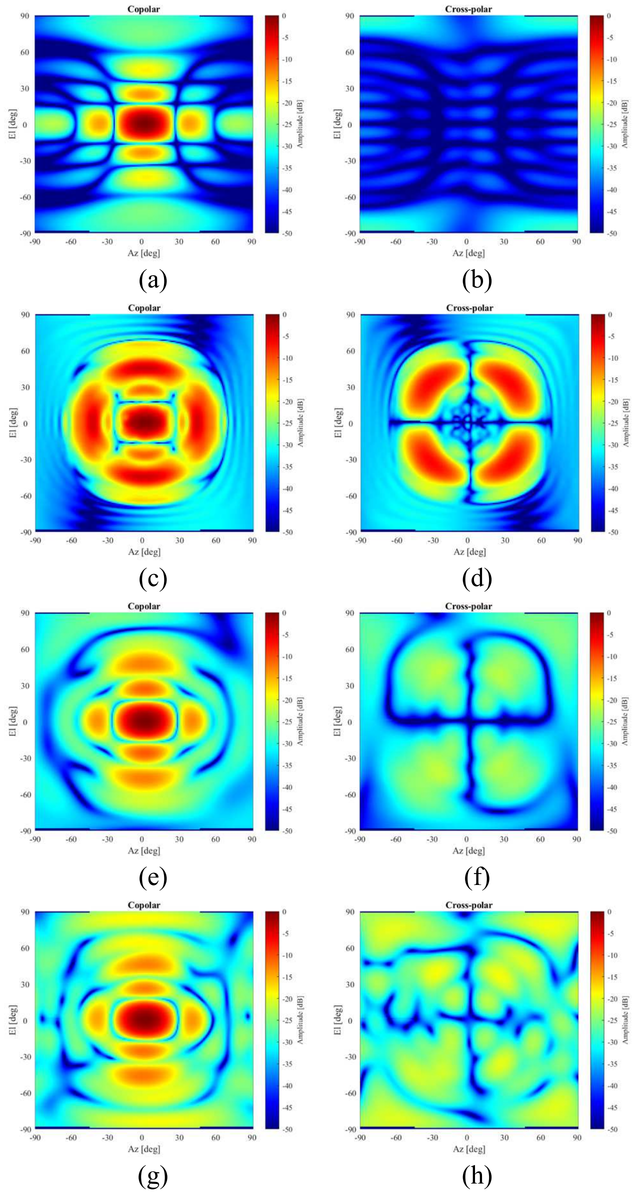

Fig. 7. Co-polar and cross-polar far-fields of the AUT obtained directly from the full wave solver in the absence of the scatterer (a) and (b); equivalent results in the presence of the PEC scatterer (c) and (d); spherical mode filtered far-field obtained using classical spherical mode filtering (e) and (f); and spherical mode filtered far-field obtained using CS based spherical mode filtering (g) and (h).

It is worth noting here that a wealth of experimental data exists that attests to the effectiveness of the underlying mode-filtering based reflection suppression technique, *cf.* [1], and thus here we have largely focused our attention on the CS recovery of the two-dimensional Fourier coefficients which is novel.

V. Conclusions

In this paper, we present the application of Compressed Sensing to spherical mode filtering for the first time. The primary objective was to effectively suppress spurious reflections in two-dimensional far-field antenna pattern measurements while significantly relaxing the sampling requirements. In this work we have demonstrated that even with sub-Nyquist sampling and data collected on a highly irregular grid, accurate antenna patterns can be recovered through sophisticated modern CS based post-processing techniques. This significantly broadens the applicability of the mode filtering approach, as it allows for reduced data acquisition time and relaxed positional equipment accuracy. This initial proof of concept shows very similar levels of performance to classical spherical mode-filtering based reflection suppression using just 8% of the number of measurement points required by classical equiangular Nyquist sampling providing a very significant reduction in terms of measurement time and a great deal of resilience to range reflections. Clearly, this is an ongoing research programme with the future work to include further verification by means of a detailed statistical analysis. Lastly, this is the first time that the NIST Fourier spherical algorithm has been harnessed for spherical processing with prior CS based spherical processing taking an equally valid, but different approach, *e.g.*, [7, 9,].

Acknowledgment

The authors would like to express their sincere thanks and appreciation to R.C. Jones for his valuable help with the EM simulation and modelling, and to Z. Chen and Y. Wang for their very valuable discussions and suggestions.

References

[1] C.G. Parini, S.F. Gregson, J. McCormick, D. Janse van Rensburg, T. Eibert, “Theory and Practice of Modern Antenna Range Measurements 2nd Expanded Edition, Volume 1”, IET Electromagnetic Waves series 55 ISBN 978-1-83953-126-2, 2021.

[2] R.C. Wittmann, C.F. Stubenrauch, “Spherical Near-Field Scanning: Experimental and Theoretical Studies”, National Institute of Standards and Technology, RL-TR-91-56, April 1991.

[3] Z. Chen, S.F. Gregson, Y. Wang, “Novel Application of Compressed Sensing in Cylindrical Mode Filtering for Far-Field Antenna Measurements”, AMTA, Seattle, Washington, October 2023.

[4] E.J. Candes, J.K. Romberg, T. Tao, “Stable Signal Recovery from Incomplete and Inaccurate Measurements”, Communications on Pure and Applied Mathematics 59, 1207–1223, 2006.

[5] D.L. Donoho, “Compressed Sensing”, IEEE Trans. Inform. Theory 52, 1289–1306, 2006.

[6] R. F. Dubrovka, R.C. Jones, C.G. Parini, S.F. Gregson, "Predication of Planar Near-Field Measurements Based on Full-Wave Three-Dimensional CEM Measurement Simulation", AMTA, Seattle, Washington, October, 2023.

[7] S.F. Gregson, C.G. Parini, “Use of Compressive Sensing Techniques for the Rapid Production Test of Commercial Nose-Mounted Radomes in a Robotic Antenna Measurement System”, AMTA, Cincinnati, October 2024.

[8] YALL1 basic solver code: Y. Zhang, J. Yang, and W. Yin. Available for download from https://github.com/andrewssobral/YALL1, last accessed 4th July 2024.

[9] R. Cornelius, D. Heberling, N. Koep, A. Behboodi and R. Mathar, “Compressed sensing applied to spherical near-field to far-field transformation,” in Proc. European Conf. Antennas Propag. (EuCAP), Davos, Switzerland, 2016, pp. 1-4.

[10] https://altair.com/feko, accessed 17/10/2024.